



Molt-dependent transcriptome analysis of claw muscles in Chinese mitten crab *Eriocheir sinensis*

Zhihuan Tian¹ · Chuanzhen Jiao¹

Received: 18 November 2018 / Accepted: 17 January 2019
© The Genetics Society of Korea 2019

Abstract

Background Molting is a critical developmental process for crustaceans, during which the claw muscles undergo periodic atrophy and restoration. But the mechanism underlying this special muscle reshuffle around ecdysis is not yet thoroughly understood.

Objective To investigate the molecular mechanism underlying the muscle's reshuffle over the molting cycle of Chinese mitten crab *Eriocheir sinensis*.

Methods The Illumina high-throughput sequencing technique were used to sequence the transcriptome of the whole claw muscles from Chinese mitten crab *Eriocheir sinensis* in three molting stages (inter-molt C stage, pre-molt D_{3–4} and post-molt A–B stage); the de novo assembly, annotation and functional evaluation of the contigs were performed with bioinformatics tools.

Results Totally 129,149 unigenes, 128,190 CDS, 33,770 SSRs and a large number of SNP sites were obtained, and 3700 and 12,771 differentially expressed genes (DEGs) were identified respectively in A–B and D_{3–4} stage compared with that in C stage. The identified DEGs were enriched to 746 and 1 408 GO terms respectively in A–B and D_{3–4} stage compared with C stage ($p \leq 0.05$). KEGG pathway analysis showed that the DEGs were significantly enriched in 14 and 11 pathways in A–B vs C comparison and D_{3–4} vs C comparison ($p \leq 0.05$), respectively. These DEGs are involved in several biological processes critical for the animal's growth and development, such as gene expression, protein synthesis, muscle development, new cuticle reconstruction, oxidation–reduction process and glycolytic process.

Conclusion The data generated in this study is the first transcriptomic resource from the muscles of Chinese mitten crab, which would facilitate to characterize key molecular processes underlying crab muscle's growth and development during the molting cycles.

Keywords Transcriptome · Molting · Claw muscle · *Eriocheir sinensis*

Introduction

Molting in crustaceans provides the basic means for growth, in which many morphological changes, such as the absorption and reconstruction of the exoskeleton (Promwikorn et al. 2005), physiological changes, such as molt-Inhibiting

hormone (Nakatsuji et al. 2000), biochemical changes, such as glycogen, lipids and inorganic elements (Tian et al. 2012), and molecular changes (Kuballa et al. 2011) have been shown to occur. Claw is a vital organ for some crustaceans such as crabs and lobsters, and it is used for moving and feeding. The claw muscles of crabs and lobsters undergo a reversible atrophy in pre-molt stage, enabling the animals to pull the large mass of claw muscle out of the narrow basi-ischial joint at ecdysis, and restored in post-molt stage (Ismail and Mykles 1992; Mykles 1997; Mykles and Skinner 1981; Schmieg et al. 1992). During this process, the thin myofilaments were preferentially removed from myofibrils before ecdysis, and the contractile devices (myofibrils) reassembled after ecdysis, which are designated as muscle reshuffle. Crustacean muscle fibres are thought

Electronic supplementary material The online version of this article (<https://doi.org/10.1007/s13258-019-00787-w>) contains supplementary material, which is available to authorized users.

✉ Chuanzhen Jiao
jiaocz@gmail.com

¹ College of Yingdong Life Science, Shaoguan University, Room C-304, Yingdong Building, No. 288, Daxue Road, Zhenjiang District, Shaoguan 512005, Guangdong, China

to grow in the time immediately after ecdysis for they must lengthen to adapt to the larger new exoskeleton (West 1997; West et al. 1995). Even though molting is a pivotal event for muscle growth in crustacean, the mechanism is not thoroughly understood yet. Crustaceans, especially those species of decapods, are important in the aquaculture and seafood industry, so the interest in their skeletal muscles' growth and development during the molt cycle is not only the pure academic but also practical.

RNA-Seq technology is a powerful tool in research on crustacean physiology for it provides a deeper and broader transcripts than other methods. Transcriptome data of crustacean in hepatopancreas (Huang et al. 2015; Lee et al. 2017), Y-organ (Das et al. 2016; Shyamal et al. 2018), hemolymph (Zhang et al. 2018), hemocytes (Qin et al. 2018), and limb bud tissue (Liu et al. 2018) have been obtained for study the development, metabolism, immune, regenerations and other biological processes of the animals. However, transcriptome data of muscles from crustacean was very limited up to now (Huang et al. 2017), and the transcriptomic variation of claw muscles related to the molting process has not yet been investigated so far.

The Chinese mitten crab *Eriocheir sinensis*, an economically important animal on aquaculture at the northern and central coast of China, is aboriginal in East Asia and an invasive species in Europe and North America (Dittel and Epifanio 2009; Wang et al. 2008). The economic and biological importance of this animal makes it a unique model for exploring the genes involved in the muscle growth over the molting. Understanding the molecular mechanism on growth and development induced by molting in *E. sinensis* could advance the aquaculture development in China and will be helpful on the control of this species in Europe or North America. In this paper, we used Illumina high-throughput sequencing and de novo assembly to establish the claw muscles' transcriptome databases of *E. sinensis*; and the annotation and functional evaluation of the contigs were also performed. This study provides the transcriptome data of claw muscles from the Chinese mitten crab during the different molting stages for the first time, and will facilitate to research on the mechanism of the muscle growth and development in crustaceans over the molting cycles.

Materials and methods

Animal sampling

The juvenile Chinese mitten crabs, weighing 8.24 ± 2.17 g, were obtained from a fisheries farm in Chongming Island (Shanghai, China), in September of 2016. Crabs of this size are very suitable for the growth and development study due to their gonads are undeveloped while the bodies are

large enough for experiment. Crabs only in inter-molt (C stage), later pre-molt (D_{3–4} stage) and early post-molt (A–B stage) were used and the molting stages were determined based on the index for *E. sinensis* described by Tian et al. (2012) (Fig. 1). Three individuals in each molting stage were sampled. The crabs were sacrificed on ice after the molting stages were identified. The whole claw muscle tissues of the crabs in C, D_{3–4} and A–B stage were collected and immediately threw into liquid nitrogen, and then transferred to -80°C for storage until the total RNA extracted.

RNA isolation and RNA-Seq library preparation

According to the manufacturer's instructions, total RNA was extracted from approximately 40 mg of claw muscle tissues using TRIzol Reagent (Sangon). The RNA integrity and quantity were tested with Qubit2.0 (Invitrogen). A total of 4 μg RNA with RNA integrity number above 7.0 was used for RNA-Seq library construction using the VAHTSTM mRNA-seq V2 Library Prep Kit for Illumina® (Vazyme, China). Three qualified RNA samples at each molting stage were then pooled and sequenced on Illumina HiseqTM2500, and produced 150 bp pair-end reads.

Transcriptome assembly and annotation

With the Fast QC program (<http://www.bioinformatics.babraham.ac.uk/projects/fastqc/>, version number 0.11.5), the quality of paired-end raw reads in fastq format were assessed. The qualified reads with a minimum phred quality score of 20 were used for further assembly. All the cleaned reads were used for the reference transcriptome assembly based on Trinity software (<https://github.com/trinityrnaseq/trinityrnaseq/wiki>, version number r20140717) (Grabherr et al. 2011). For annotation, the assembled transcripts (unigenes) were Blast (blastX or Blastn) search against the databases of NR, NT, CDD, Swiss-Prot, GO, KOG, PFAM, TrEMBL and KEGG with a cut off E value of $1e-5$.

Identification of CDS, SSR and SNP

The protein-coding DNA sequence region (CDS) was predicted using OrfPredictor software (<http://bioinformatics.yzu.edu/tools/OrfPredictor.html>, version number 1.0) with default parameters. The software MISA (<http://pgrc.ipk-gatersleben.de/misa/>, version number 1.0) was used to predict simple sequence repeat (SSR) and microsatellite markers in the assembled sequences. The identification of perfect mono-, di-, tri-, tetra-, penta-, and hexa-nucleotide motifs with a minimum of 10, 6, 5, 5, and 5 repeats, respectively were performed. Only SSRs with flanking sequences longer

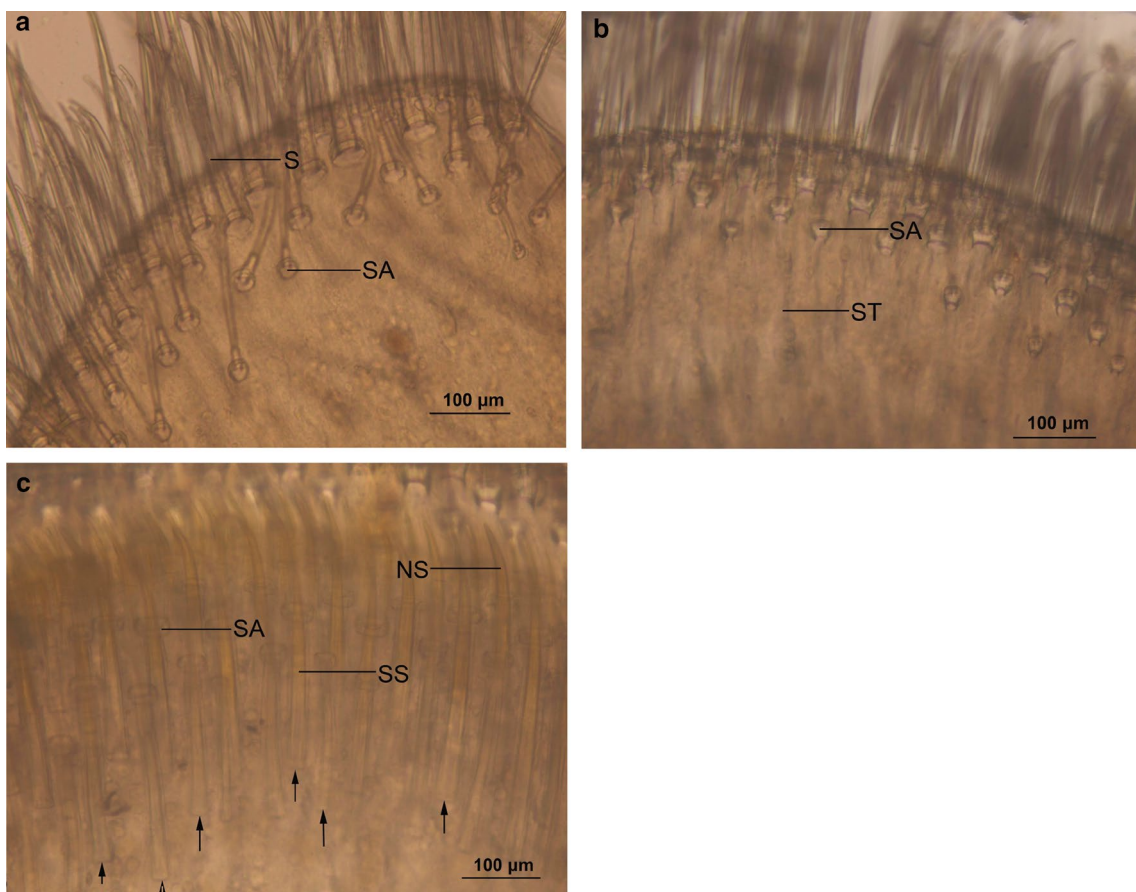


Fig. 1 Morphological changes of basal endite of the second maxilla of *E. sinensis* in post-molt A–B stage (**a**), inter-molt C stage (**b**), and pre-molt D_{3–4} stage (**c**) under a light microscope. Observed physical characteristics of each stage were as follows: **a** post-molt A–B stage: formation of the cuticle is incomplete and the setal track under the setal articulation (SA) is not distinguishable. **b** Inter-molt C stage:

cuticular formation is complete, showing a setal track (ST) under the setal articulation (SA). **c** Later pre-molt D_{3–4} stage: the setal articulations (SA) are completed and the proximal ends of the setal shafts are closed (arrowheads). *S* seta, *NS* new setae, *SS* setal shaft (Tian et al. 2012)

than 50 bps on both sides were collected for future marker development. The candidate single nucleotide polymorphism (SNP) were identified in the assembled sequences using Samtools software (<http://samtools.sourceforge.net/>, version number 0.1.18) (Li et al. 2009).

Transcript abundance estimation and statistical analyses

Gene expression levels were valued with RSEM software (<http://deweylab.biostat.wisc.edu/rsem/>, version number 1.0) (Li and Dewey 2011) based on read counts, and then normalized with the FPKM (Fragments Per Kilo bases per Million fragments) transformation (Mortazavi et al. 2008). Further data processing and statistical analysis were performed using R statistical software (<http://www.r-project.org>, version number 1.0). Differentially expressed genes (DEGs) were identified using the method established by Audic and Claverie, and then performed multiple hypothesis testing

using false discovery rate (FDR) (Audic and Claverie 1997; Benjamini and Yekutieli 2001). A threshold of $P \leq 0.01$ and Fold change > 2 were set for significance differences of gene expression between comparable samples (A–B vs C and D_{3–4} vs C comparisons).

GO and KEGG analysis of differentially expressed genes

The differentially expressed genes were assigned to terms in the GO database (<http://www.geneontology.org>), and then the numbers of genes for each term were determined, after which a hypergeometric test was used to select significantly enriched GO terms (Young et al. 2010). The KEGG database (<http://www.kegg.jp/>) was used to assign and predict putative functions and pathways associated with the assembled sequences (Kanehisa et al. 2008). A heat map which grouped genes according to FPKM values was generated in Cluster 3.0

(de Hoon et al. 2004) and visualized in TreeView 1.6 to analyze their expression levels across molting periods (Saldanha 2004).

Data availability

The sequence data in this paper have been deposited into the NCBI Sequence Read Archive (<http://trace.ncbi.nlm.nih.gov/Traces/sra/sra.cgi?view=studies>), and the accession numbers of the three samples are SRR7984118, SRR7984119, and SRR7984120.

Results

Transcriptome assembly

After removing the adaptors and filtering, we obtained 47,593,937, 4,865,6041 and 58,184,040 qualified paired-end reads from the C, A–B and D_{3–4} molting stages cDNA libraries of the claw muscles respectively. All the qualified reads were combined and assembled de novo with paired-end methods, resulting in 149,248 transcripts or 129,149 unigenes with the length of more than 200 bp (Table 1). Approximately 76.40%, 71.90% and 76.15% of clean reads aligned back to the assembled transcripts in C, A–B, and D_{3–4} cDNA libraries.

Functional annotation

The 129,149 unigenes were used to Blast (BlastX or Blastn) search against the databases of NR, NT, CDD, Swiss-Prot, GO, KOG, PFAM, TrEMBL and KEGG. Of all the Unigenes, 57,994 (44.9%) were annotated in at least one of the above databases, and 1198 (0.93%) were annotated in all the databases (Table 2). GO analysis showed that 32,835 unigenes were mapped to at least one GO category and more unigenes were mapped to the GO terms of cellular and metabolic processes, cell and cell part, binding and catalytic activity (Fig. 2a). The KEGG pathways identified through the functional analysis of the unigenes were shown in Fig. 2b, in which the signal transduction has the most unigenes (4074), followed by endocrine system (2124) and carbohydrate metabolism (2047). Based on KOG database, the most unigenes (3063) were annotated as general function prediction only (R), 2809 unigenes were annotated as signal transduction mechanisms (T), and 2147 unigenes were annotated as posttranslational modification, protein turnover and chaperones (O) (Fig. 2c).

Table 1 Information of transcriptome assembly

	All number	≥ 500 bp	≥ 1000 bp	N50	N90	Max length	Min length	All length	Mean length
Transcript	149,248	47,212	22,324	974	257	17,794	201	93,579,761	627.01
Unigene	129,149	35,191	14,912	728	245	17,794	201	71,027,035	549.96

Table 2 Information of unigenes annotated in each database

Database	Number of unigenes	Percentage (%)
Annotated in CDD	30,305	23.47
Annotated in KOG	23,076	17.87
Annotated in NR	37,474	29.02
Annotated in NT	21,106	16.34
Annotated in PFAM	26,641	20.63
Annotated in Swissprot	33,242	25.74
Annotated in TrEMBL	38,484	29.8
Annotated in GO	32,835	25.42
Annotated in KEGG	18,400	14.25
Annotated in at least one database	57,994	44.9
Annotated in all database	1198	0.93
Total Unigenes	129,149	100

CDS, SSR and SNP analysis

There are 128,190 CDS predicted from all the 129,149 unigenes. The top3 CDS numbers fall into sequence size of 100–200 (bp), 200–300 (bp) and 300–400 (bp). As the sequence size increases, the number of CDS predicted is decreasing. A total of 1 648 CDS larger than 2000 bp were predicted altogether (Fig. 3). A total of 33,770 SSRs were predicted from 129,149 assembled transcripts with the total size of 71,027,035 bp. The repeat nucleic acids ranges from 1 to 6 bp, and the most SSRs were 2-nucleotide repeats (14,623), followed by 3-nucleotide repeats (10,057) and 1-nucleotide repeats (8279) (Online Resource 1). The density of 2-nucleotide repeats was the largest (205.88 per Mb), followed by 3-nucleotide repeats (141.59 per Mb) and 1-nucleotide (116.56 per Mb) (Fig. 4). All the SSRs and their suggested primers were listed in online resource 2. A total number of 97,107, 94,046 and 139,647 possible SNPs were obtained from the molting stage C, A–B and D_{3–4} respectively, the most common nucleotide changes in all the three stages are C: G–T: A, followed by T: A–C: G. All the predicted SNPs were listed in online resource 3.

Fig. 2 Functional annotation of the unigenes in GO (**a**), KEGG (**b**) and KOG (**c**) databases

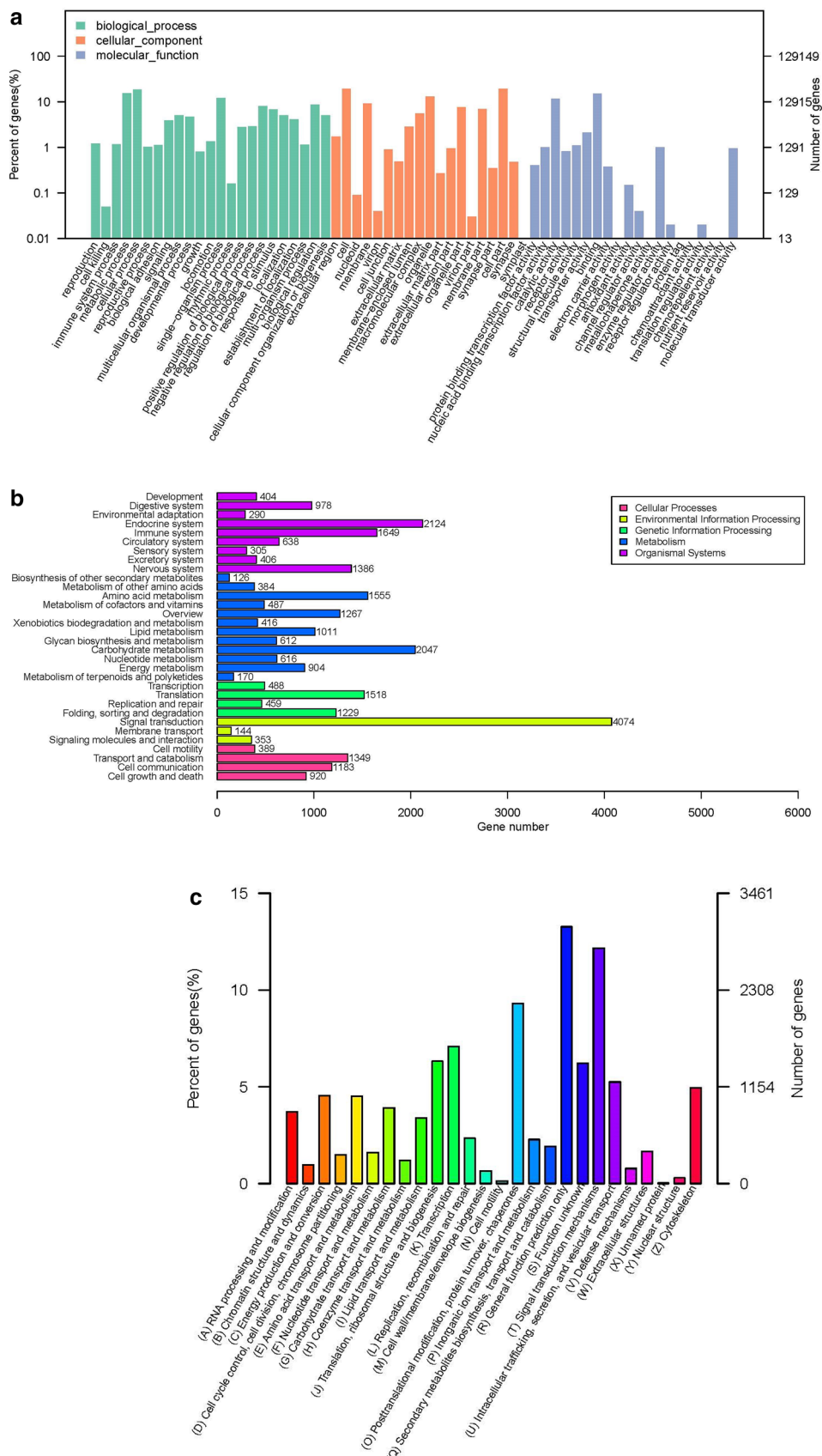


Fig. 3 The distribution of CDS Length

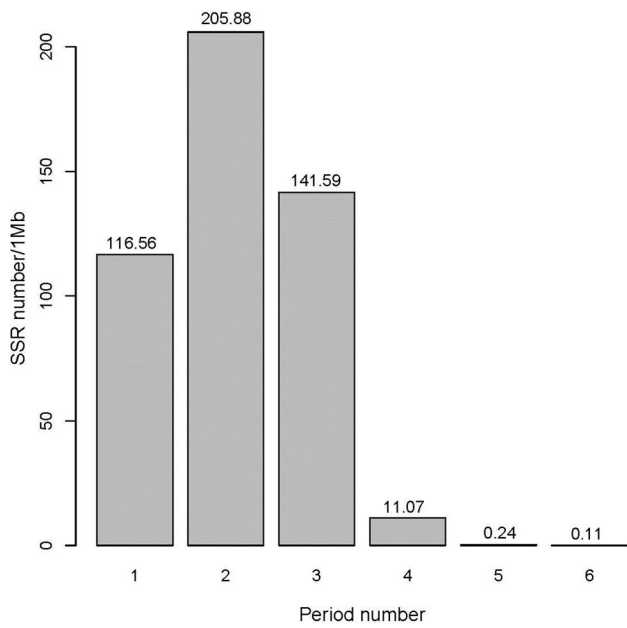
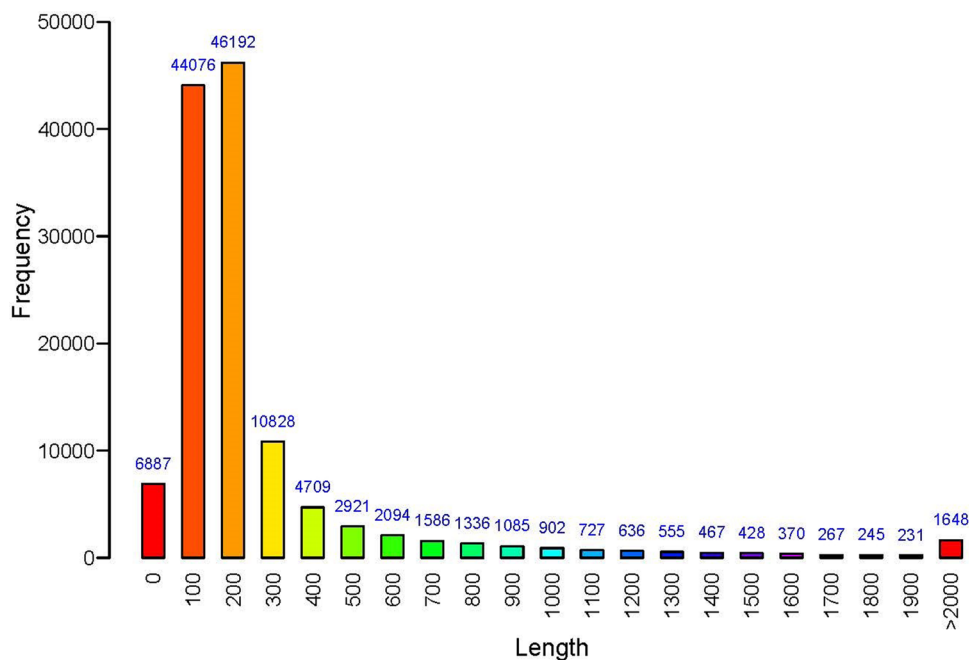


Fig. 4 The distribution of SSR density

Differentially expressed genes (DEGs) among muscle tissues of the crabs in C, D_{3–4} and A–B molting stages

There were different amounts of unigenes expressed in the claw muscles of A–B, C, and D_{3–4} molting stages. The largest number of assembled unigenes exclusively expressed in D_{3–4} stage (34,834), followed by C stage (6938) and A–B stage (5466) respectively. A total of 3700 and 12,771

differentially expressed genes (DEGs) were identified in A–B and D_{3–4} stage compared with that in C stage, among which 1898 genes (1037 up regulated and 313 down regulated) were differentially expressed both in A–B stage and D_{3–4} stage compared with C stage (Fig. 5). Some differentially expressed genes among the three samples were listed in Table 3. To further classify and predict the function of DEGs, we performed hierarchical clustering of these genes from the three samples. The 14,573 differentially expressed genes with the same regulation pattern were clustered into 14 sub-clusters. The largest group, sub-cluster 1, contains 6126 DEGs with gene expression levels increasing its maximum in pre-molt D_{3–4} stage, and begin decreasing from post molt A–B stage till inter-molt C stage. Other sub-clusters containing over 300 members were sub-cluster 3 (5937 DEGs), sub-cluster 4 (1013 DEGs), sub-cluster 2 (617 DEGs), and sub-cluster 5 (487 DEGs) (Online Resource 4).

GO enrichment analysis of DEGs from three molting stages

The DEGs in A–B vs C comparison were enriched to 746 GO terms ($p \leq 0.05$), of which 489 (56.5%) belong to biological process (BP), 167 (22.4%) belong to molecular function (MF) and 90 (12.1%) belong to cellular component (CC). The up regulated DEGs in A–B stage compared with that in C stage are enriched in GO terms as structural constituent of cuticle (GO0042302), nucleolus (GO0005730), ribosome biogenesis (GO0042254), ribonucleoprotein complex biogenesis (GO0022613) and rRNA processing (GO0006364). For those down regulated DEGs in A–B stage, their detailed

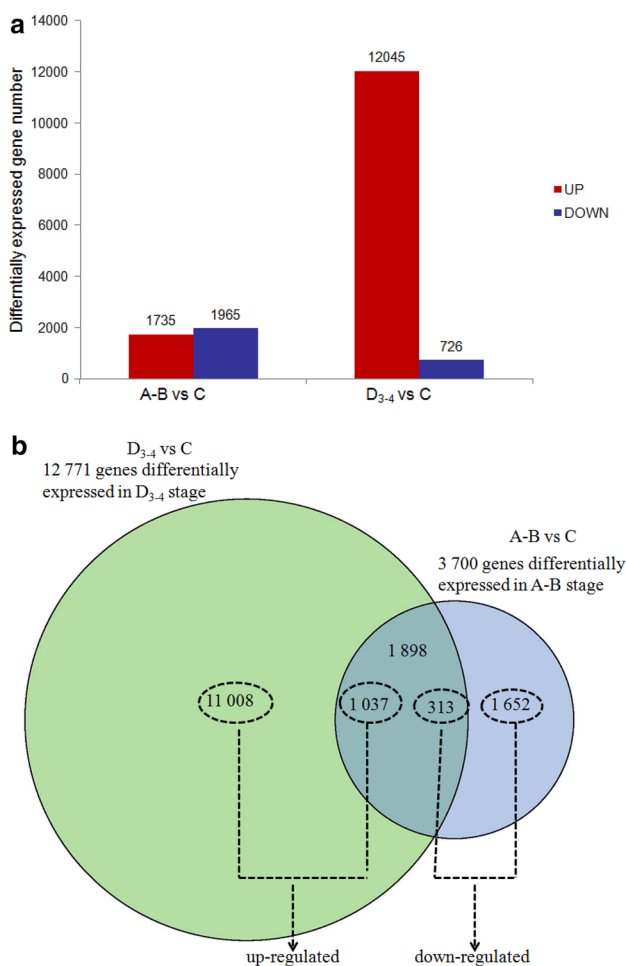


Fig. 5 Information of differentially expression genes (DEGs) among the three molting stages. **a** The amount of DEGs in A–B and D_{3–4} stage compared with that in C stage. **b** The Venn diagrams of DEGs. Each circle represent the differentially expressed genes within each comparative group and circle overlap represents the number of the differentially expressed genes both in the two comparative group

functions are enriched in GO terms as mitochondrial inner membrane (GO0005743), electron transport chain (GO002290), oxidation–reduction process (GO0055114), and oxidoreductase activity (GO0016491).

There were 1 408 enriched GO terms from D_{3–4} vs C comparison, of which 1 117 (79.4%) belong to BP, 158 (11.2%) belong to MF and 133 (9.4%) belong to CC. The up regulated DEGs in D3-4 stage, compared with C stage, function in nucleus (GO0005634), involved in RNA processing (GO0006396), gene expression (GO0010467) and structural constituent of cuticle (GO0042302). Those down regulated DEGs in D3-4 stage, the enriched GO terms include mitochondrial inner membrane (GO0005743), carbohydrate metabolic process (GO0005975), structural constituent of cuticle (GO0042302), sarcomere (GO0030017), contractile fiber part (GO0044449), myofibril (GO0030016), Z disc

(GO0030018) and I band (GO0031674). The top 15 (based on P values) enriched GO terms by those up/down-regulated DEGs in A–B and D_{3–4} stage compared with C stage were listed in Table 4.

KEGG pathway analysis of the DEGs from three molting stages

With the KEGG pathway analysis we further investigated the interactions among DEGs in their functioning in the biological processes. it showed that the differentially expressed genes were altogether enriched in 282 pathways in A–B vs C comparison and 302 in D_{3–4} vs C comparison, among which 14 and 11 pathways were significantly enriched ($p \leq 0.05$) respectively (Table 5). Between A–B and C stage, the DEGs belong to hedgehog signaling pathway (ko04340) is the most prominent, following by arachidonic acid metabolism (ko00590), ubiquitin mediated proteolysis (ko04120), RNA transport (ko03013) and glutathione metabolism (ko00480).The significantly enriched KEGG pathways between C and D_{3–4} stages are ribosome biogenesis in eukaryotes (ko03008), ubiquitin mediated proteolysis (ko04120), cytosolic DNA-sensing pathway (ko04623), RNA transport (ko03013), and RNA polymerase (ko03020). The Heat-map of the enriched KEGG pathways of DEGs among the 3 stages was showed in Fig. 6.

Discussion

Due to the rapid advancement of sequencing technology, there are more and more genomic and transcriptome data of crustaceans available in the public bioinformatics database. Up to now, high-coverage genomes of the cladoceran *Daphnia pulex* (Colbourne et al. 2011), the amphipod *Parhyale hawaiensis* (Kao et al. 2016), and the decapoda *Procambarus virginalis* (Gutekunst et al. 2018) had been sequenced. Several genomes of economically important crustaceans of decapoda, such as the penaeid shrimps *Penaeus monodon* and *Marsupenaeus japonicus* (Yuan et al. 2018), the caridean shrimps *Neocaridina denticulata* (Kenny et al. 2014) and *Exopalaemon carinicauda* (Yuan et al. 2017), and the crab *Eriocheir sinensis* (Song et al. 2016), although in low coverage, were also published. Transcriptome from tissues such as hepatopancreas, gills, haemocytes, testis, et al. under different development stages, environmental conditions, pathogens challenges, et al. were performed by different researchers; and the data are available in public databases (<https://www.ncbi.nlm.nih.gov/sra/>). As a vital organ used for move and predation by crabs and lobsters, the claw muscles undergo reversible atrophy before ecdysis. The mechanism of this special muscle's reshuffle was not

Table 3 Part of differentially expressed genes in A–B and D_{3–4} stage compared with C stage

Comparison	Gene ID	Expression	Name	Description
A-B vs C	c120758_g1	Up	<i>Calcified cuticle protein cp19.0</i>	Structural constituent of cuticle
	c121510_g1	Up	<i>Cuticular protein 34</i>	Structural constituent of cuticle
	c14581_g1	Up	<i>Putative nuclease harbi1</i>	Nuclease
	c20216_g1	Up	<i>Arthrodial cuticle protein amp8.1</i>	Structural constituent of cuticle
	c21554_g1	Up	<i>V-type proton atpase subunit f</i>	Proton-transporting v-type atpase, v1 domain
	c21989_g1	Up	<i>Cuticle protein amp1a</i>	Structural constituent of cuticle
	c24241_g1	Up	<i>Gastrolith protein 59</i>	Protein glycosylation
	c27028_g1	Up	<i>Fushi tarazu-factor 1</i>	Steroid hormone receptor activity
	c27065_g1	Up	<i>Protein hexim</i>	Negative regulation of transcription from rna polymerase ii
	c29083_g1	Up	<i>Cuticular protein 15</i>	Structural constituent of cuticle
	c18480_g1	Down	<i>Fructose-bisphosphate aldolase</i>	Fructose-bisphosphate aldolase activity
	c24865_g1	Down	<i>Putative atp synthase subunit</i>	Atp biosynthetic process
	c28513_g1	Down	<i>Glyceraldehyde 3-phosphate dehydrogenase</i>	Glucose metabolic process
	c31277_g1	Down	<i>Lim domain and actin-binding protein 1-like</i>	Actin filament binding
	c32162_g2	Down	<i>Muscle lim protein 1</i>	Muscle tissue development
	c32184_g1	Down	<i>Cytochrome b</i>	Respiratory chain
	c32418_g1	Down	<i>Heat shock protein beta-1</i>	Response to stress
	c33042_g1	Down	<i>Triosephosphate isomerase</i>	Gluconeogenesis
	c33160_g1	Down	<i>Phosphoglycerate mutase 2</i>	Gluconeogenesis
D _{3–4} vs C	c33481_g1	Down	<i>Malate dehydrogenase</i>	Cellular carbohydrate metabolic process
	c10339_g1	Up	<i>Beta-i tubulin</i>	Microtubule-based movement
	c106124_g1	Up	<i>40s ribosomal protein s18-like</i>	Translation
	c106254_g1	Up	<i>Transketolase</i>	Ribose phosphate biosynthetic process
	c106571_g1	Up	<i>Cuticlin-1</i>	Structural constituent of cuticle
	c107286_g1	Up	<i>40s ribosomal protein s13</i>	Translation
	c109028_g1	Up	<i>Checkpoint serine/threonine-protein kinase bub1-like</i>	Mitosis
	c109347_g1	Up	<i>Ribosomal protein s3a</i>	Translation
	c109358_g1	Up	<i>Peroxiredoxin</i>	Antioxidant activity
	c110508_g1	Up	<i>Adult beta globin</i>	Hemoglobin subunit beta-2
	c110601_g1	Up	<i>60s ribosomal protein l21</i>	Srp-dependent cotranslational protein
	c12727_g1	Down	<i>Four and a half lim domains protein 2</i>	Negative regulation of transcription from rna polymerase ii promoter
	c17092_g1	Down	<i>Muscle lim protein mlp84b-like</i>	Muscle tissue development
	c17646_g1	Down	<i>Malate dehydrogenase</i>	Tricarboxylic acid cycle
	c18480_g1	Down	<i>Fructose-bisphosphate aldolase</i>	Glycolysis
	c28021_g1	Down	<i>F1f0-atp synthase beta subunit</i>	Hydrogen-exporting atpase activity
	c28513_g1	Down	<i>Glyceraldehyde 3-phosphate dehydrogenase</i>	Glucose metabolic process
	c31277_g1	Down	<i>Lim domain and actin-binding protein 1-like</i>	Actin filament binding
	c31540_g1	Down	<i>Fructose 1,6-bisphosphatase</i>	Gluconeogenesis
	c32160_g1	Down	<i>Protein tob2</i>	Anti-proliferative protein
	c33042_g1	Down	<i>Triosephosphate isomerase</i>	Gluconeogenesis

P≤0.01 and fold change>2

clear yet and no related transcriptome data available up to now. This study provided comprehensive sequence data of annotated genes, DEGs, SSRs, and SNPs for the claw muscle tissues of *E. sinensis* in three different molting stages. These data are the start point to investigate the

molecular mechanisms of muscle changes in the molting cycle of the crab, and we also give some clues to this topic based on the functional analysis of these data.

Table 4 The top 10 GO terms of differentially expressed genes (DEGs) enriched in A-B and D₃₋₄ stage compared with C stage

Comparison	GO ID	Term	Type	DEGs in this term	P value	Expression
A-B vs C	GO 0042302	Structural constituent of cuticle	Molecular function	36	1.00E-30	Up
	GO 0005730	Nucleolus	Cellular component	84	1.40E-25	Up
	GO 0042254	Ribosome biogenesis	Biological process	42	1.50E-16	Up
	GO 0022613	Ribonucleoprotein complex biogenesis	Biological process	46	6.20E-15	Up
	GO 0031981	Nuclear lumen	Cellular component	123	3.10E-14	Up
	GO 0034660	lncRNA metabolic process	Biological process	56	4.30E-14	Up
	GO 0044428	Nuclear part	Cellular component	144	1.70E-12	Up
	GO 0005634	Nucleus	Cellular component	279	7.50E-11	Up
	GO 0006364	rRNA processing	Biological process	27	2.70E-10	Up
	GO 0016072	rRNA metabolic process	Biological process	27	6.40E-10	Up
	GO 0005739	Mitochondrion	Cellular component	186	1.00E-30	Down
	GO 0044429	Mitochondrial part	Cellular component	125	1.00E-30	Down
	GO 0005740	Mitochondrial envelope	Cellular component	88	3.90E-25	Down
	GO 0031966	Mitochondrial membrane	Cellular component	86	6.40E-25	Down
	GO 0005743	Mitochondrial inner membrane	Cellular component	72	2.90E-23	Down
	GO 0019866	Organelle inner membrane	Cellular component	72	6.20E-22	Down
	GO 0044444	Cytoplasmic part	Cellular component	332	1.50E-20	Down
	GO 0031967	Organelle envelope	Cellular component	93	1.00E-17	Down
	GO 0070469	Respiratory chain	Cellular component	37	4.60E-17	Down
	GO 0006091	Generation of precursor metabolites and energy	Biological process	70	1.90E-15	Down
D ₃₋₄ vs C	GO 0005634	Nucleus	Cellular component	1715	1.00E-30	Up
	GO 0043226	Organelle	Cellular component	2956	1.00E-30	Up
	GO 0043227	Membrane-bounded organelle	Cellular component	2631	1.00E-30	Up
	GO 0043229	Intracellular organelle	Cellular component	2942	1.00E-30	Up
	GO 0043231	Intracellular membrane-bounded organelle	Cellular component	2625	1.00E-30	Up
	GO 0044428	Nuclear part	Cellular component	767	1.00E-30	Up
	GO 0031981	Nuclear lumen	Cellular component	592	1.10E-28	Up
	GO 0044446	Intracellular organelle part	Cellular component	1748	4.80E-27	Up
	GO 0006396	RNA processing	Biological process	345	1.90E-26	Up
	GO 0044424	Intracellular part	Cellular component	3372	2.30E-26	Up
	GO 0006091	Generation of precursor metabolites and energy	Biological process	42	1.60E-16	Down
	GO 0005739	Mitochondrion	Cellular component	64	5.90E-15	Down
	GO 0044429	Mitochondrial part	Cellular component	44	9.70E-14	Down
	GO 0042302	Structural constituent of cuticle	Molecular function	13	1.30E-11	Down
	GO 0005743	Mitochondrial inner membrane	Cellular component	29	3.80E-11	Down
	GO 0030017	Sarcomere	Cellular component	16	9.40E-11	Down
	GO 0019866	Organelle inner membrane	Cellular component	29	1.30E-10	Down
	GO 0030018	Z disc	Cellular component	13	1.80E-10	Down
	GO 0031966	Mitochondrial membrane	Cellular component	32	2.80E-10	Down
	GO 0031674	I band	Cellular component	13	3.20E-10	Down

Transcriptomic variation among claw muscles from different molting stages

We selected three typical molting stages (inter-molt C stage, later pre-molt D₃₋₄ stage and post-molt A-B stage) of *E. sinensis* to investigate the transcriptomic variation among claw muscles. A large number of annotated unigenes were

attained for each transcriptome. The most numbers of assembled unigenes were found in D₃₋₄ stage, followed by that in C stage. These are two critical periods that may have more genes respond to developmental and physiological changes over the molt cycle as discussed below.

Shedding off the old cuticle leaves the crustacean a larger and soft body. Post-molt A-B stage is the beginning of a

Table 5 The significantly enriched KEGG pathways of differentially expressed genes (DEGs) in A–B and D_{3–4} stages compared with C stage

Comparison	KO ID	Term	Type	DEGs in this term	UP	Down	P value
A-B vs C	ko04340	Hedgehog signaling pathway	Environmental information processing	7	6	1	0.008266
	ko00590	Arachidonic acid metabolism	Metabolism	6	4	2	0.015822
	ko04120	Ubiquitin mediated proteolysis	Genetic information processing	17	8	9	0.015826
	ko03013	RNA transport	Genetic information processing	23	8	15	0.018548
	ko00480	Glutathione metabolism	Metabolism	11	7	4	0.020082
	ko05033	Nicotine addiction	Human diseases	2	1	1	0.030043
	ko00311	Penicillin and cephalosporin biosynthesis	Metabolism	1	0	1	0.035186
	ko00472	D-Arginine and D-ornithine metabolism	Metabolism	1	0	1	0.035186
	ko00624	Polycyclic aromatic hydrocarbon degradation	Metabolism	1	0	1	0.035186
	ko00901	Indole alkaloid biosynthesis	Metabolism	1	0	1	0.035186
	ko00281	Geraniol degradation	Metabolism	2	2	0	0.037741
	ko00982	Drug metabolism-cytochrome P450	Metabolism	5	3	2	0.040641
	ko03040	Spliceosome	Genetic information processing	20	7	13	0.041393
	ko04140	Regulation of autophagy	Cellular processes	4	2	2	0.04715
D _{3–4} vs C	ko03008	Ribosome biogenesis in eukaryotes	Genetic information processing	33	32	1	0.00018
	ko04120	Ubiquitin mediated proteolysis	Genetic information processing	45	41	4	0.00081
	ko04623	Cytosolic DNA-sensing pathway	Organismal systems	12	12	0	0.00148
	ko03013	RNA transport	Genetic information processing	61	54	7	0.00176
	ko03020	RNA polymerase	Genetic information processing	13	13	0	0.00311
	ko03450	Non-homologous end-joining	Genetic information processing	8	8	0	0.0057
	ko00590	Arachidonic acid metabolism	Metabolism	12	8	4	0.01328
	ko03022	Basal transcription factors	Genetic information processing	12	11	1	0.01516
	ko03015	mRNA surveillance pathway	Genetic information processing	29	23	6	0.02576
	ko00532	Glycosaminoglycan biosynthesis-chondroitin sulfate/dermatan sulfate	Metabolism	8	8	0	0.02668
	ko03440	Homologous recombination	Genetic information processing	10	9	1	0.03625

molting cycle, a period in which the animal is recovering from molting and its exoskeleton is quickly hardened to avoid predation. The highly expressed gene in this stage compared that with in C stage are associated with structural constituent of cuticle, such as *calcified cuticle protein CP19.0*, *cuticular protein 34*, *arthrodial cuticle protein AMP8.1*, *Cuticle protein AMP1A* and *cuticular protein 15*. As is known, the syntheses of the endo-cuticle and membranous layer of the new cuticle proceed chronologically after the ecdysis, accompanied with the calcification of new cuticle (Promwikorn et al. 2005). When the synthesis and calcification of the new cuticles are complete, the animal enter into the inter-molt stage. Consistent with the physical changes above, the most significantly enriched GO terms by up regulated DEGs in this stage is structural constituent of cuticle, which involved in construction and calcification of the new cuticle.

The dissolved myofilaments of claw muscles in later pre-molt of last molting cycle are also reassembled in this stage. Crustacean muscle fibres are believed to grow in the

period of immediately after ecdysis, when they elongate to accommodate the new larger exoskeleton (West 1997; West et al. 1995). In American lobster, *Homarus americanus*, the claw muscles maintain an elevated ribosomal activity in the post-molt stage (El Haj et al. 1996). The transcriptome data in this study showed that some of the up-regulated DEGs in A–B stage were enriched in GO terms as rRNA processing, aminoacyl-tRNA ligase activity and aminoacyl-tRNA ligase activity, which are involved in translation. This result is consistent with the report that the protein synthesis rate in pos-molt A–B stage increased compared with that in C stage, and the increased proteins such as sarcomeric proteins were used to rebuild the eroded contractile elements and provide materials for subsequent muscle growth (Mykles and Skinner 1990; Whiteley and El Haj 1997). In addition, the prominent down-regulated DEGs in A–B stage enriched in GO terms including mitochondrial inner membrane, electron transport chain, cellular amino acid catabolic process and cytochrome-coxidase activity in this study. These results are in accordance with the low level of energy metabolism of the

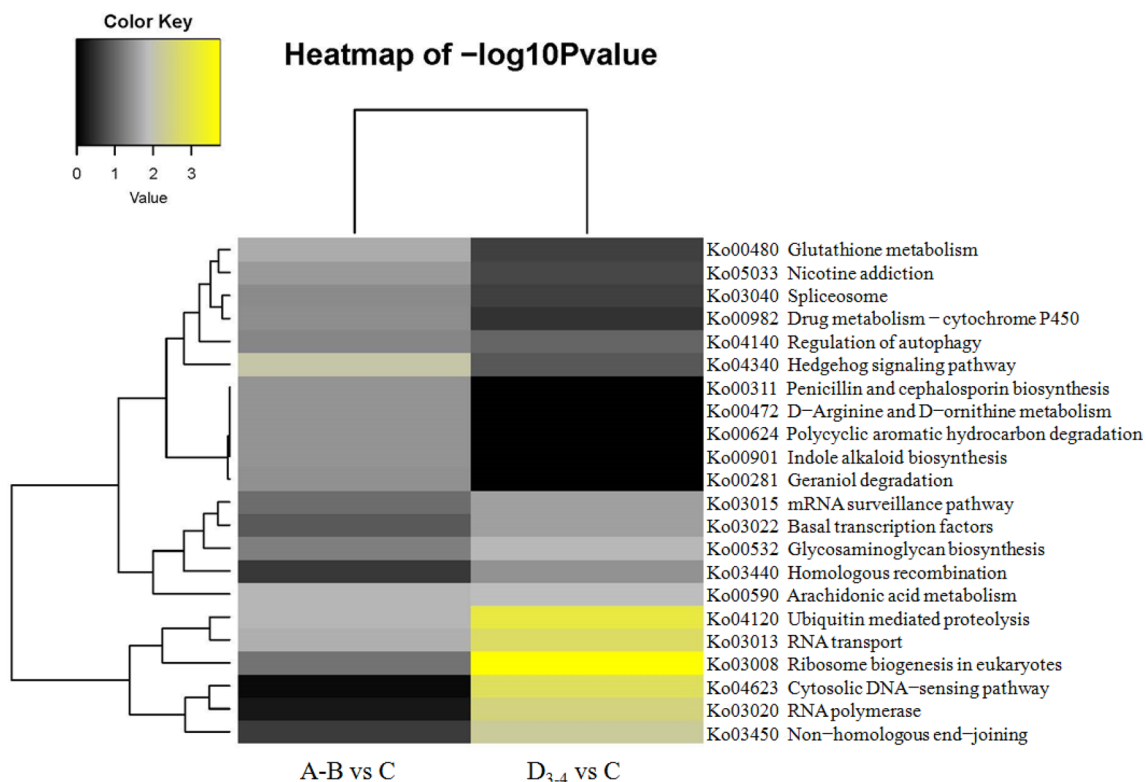


Fig. 6 Heat-map of the enriched KEGG pathways of differentially expression genes among the three molting stages

newly molters, which are not active in feeding and moving when they just finished the ecdysis.

The KEGG analysis help us to investigate the biochemical metabolisms and signal transduction pathways of the DEGs involved. In A–B stage, the DEGs enriched in KEGG that relatively significant was hedgehog signaling pathway, followed by arachidonic acid metabolism, ubiquitin mediated proteolysis, RNA transport, glutathione metabolism successively, which indicate a higher protein synthesis activity in this stage, and thereby starting a new round of growth and development in the following stage.

The following inter-molt C stage is the main period of growth and development for crustaceans, and the animals in this stage are active in feeding and moving (Devaraj and Natarajan 2006; Huang et al. 2015; Tian et al. 2012). A number of highly expressed genes identified in this stage compared with A–B or D_{3–4} stage are associated with the glycolysis and gluconeogenesis, such as *fructose 1,6-bisphosphatase*, *glyceraldehyde 3-phosphate dehydrogenase*, *fructose-bisphosphate aldolase*, *triosephosphate isomerase*, *phosphoglycerate mutase 2* and *triosephosphate isomerase*. Pyruvic acid, a product of glycolysis, could provide energy for cells through citric acid cycle under aerobic conditions and consequently promote the growth and development of *E. sinensis* in C stage, while gluconeogenesis ensures that the animal's blood sugar keeping at normal levels. Other highly

expressed genes are associate with the respiratory metabolism (such as *FIFO-ATP synthase beta subunit*, *cytochrome b* and *putative ATP synthase subunit*) and muscle tissues development (such as *Muscle LIM protein 1* and *Muscle LIM protein Mlp84B-like*), indicating that the animals' metabolism and muscles growth are undergoing at a relative high level in this period.

The pre-molt D stage is a critical phase in a molting cycle in crustacean, during which the crabs are preparing for ecdysis. In later pre-molt D_{3–4} stage, the claw muscles myofilaments dissolved to make the muscles pulled out of the narrow basi-ischial joint (Mykles and Skinner 1981; West et al. 1995), while the protein synthesis rate was still increased in the atrophied muscles compared with that in the inter-molt C stage (El Haj et al. 1996; El Haj 1999). This may account for the increases in the production of degradative enzymes as Mykles suggested (Mykles 1999; Mykles and Skinner 1990; Yu and Mykles 2003). In the lobster, the increases in protein synthesis was not due to the increased ribosome numbers, it's the result of the increased ribosome activity, increased transcription and mRNA production in the atrophied muscle (El Haj et al. 1996; El Haj 1999). Another significant change over a molt cycle is the cuticular degradation and reconstruction. During the pre-molt period, the old cuticles separated from epidermis and the new epicuticles and exocuticles (pre-ecdysial cuticle) were synthesized inside of the

old ones in D_{3–4} stage (Promwikorn et al. 2005). Consistently, it is showed that many genes highly expressed in the D_{3–4} stage (compared with that in C stage) are most likely involved in the physiological events above mentioned in this stage. For example, the highly expressed *beta-I tubulin* gene is associated with microtubule-based movement; *checkpoint serine/threonine-protein kinase BUB1* gene is associated with mitosis; *Cuticlin-1* gene is associated with structural constituent of cuticle; and *transketolase*, *40S ribosomal protein S13*, *40S ribosomal protein S18-like*, *ribosomal protein S3a* and *60S ribosomal protein L21* genes are involved in ribose phosphate biosynthetic process and protein translation.

The enriched GO terms by up-regulated DEGs in D_{3–4} stage are involved in RNA metabolic process, such as mRNA processing and RNA binding, and structural constituent of cuticle, indicating that the high active of gene expression, protein synthesis, and new cuticle reconstruction are in progress in this stage. Those down-regulated DEGs were enriched in GO terms of mitochondrial inner membrane, sarcomere, oxidation-reduction process, glycolytic process, transaminase activity, structural constituent of cuticle, muscle alpha-actinin binding, Z disc, and I band in D_{3–4} stage. These data would explain the mechanisms under which the low activity, low energy consumer, and the myofilament dissolution in the later pre-molt period when the animals were fasting and motionless.

The enriched KEGG pathways by DEGs in D_{3–4} stage compared with C stage are ribosome biogenesis in eukaryotes, RNA transport, cytosolic DNA-sensing pathway and RNA polymerase, indicating the high active of gene expression and protein synthesis as GO analysis predicated. The ubiquitin mediated proteolysis pathway (ko04120) was also enriched prominently in this stage (Fig. 6). It is known that ubiquitin involved in protein degradation, muscle atrophy, stage-specific development, and programmed cell death (Haas et al. 1995; Mykles 1998; Pickart et al. 2010; Wing and Goldberg 1993). The prominent enriched ubiquitin mediated proteolysis pathway in D_{3–4} stage indicate its participation in the dissolution and rearrangement of myofilaments in claw muscle induced by molting. It has been observed that polyubiquitin mRNA, ubiquitin-protein conjugates, and the proteasome activity in the atrophied claw muscles increased in the later pre-molt stage of *Gecarcinus lateralis* and *Homarus americanus* (Koenders et al. 2002; Shean and Mykles 1995; Spees et al. 2003).

Although the transcriptome data from the claw muscles were obtained, and their variations among the three molting stages were analyzed in this study, the key regulators which may control the muscles' growth and reshuffling around ecdysis, and which are mostly hidden in the DEGs reported in this study, are needed to be further identified and validated, and this will thus be the focus of our future research.

In conclusion, the comprehensive transcriptome study on claw muscles of *E. sinensis* from three molting stages was performed in this article, and the transcriptome data as well as the annotated assembly transcripts were given here. The differently expressed genes, especially those muscle-related such as *Muscle LIM protein Mlp84B-like*, *Muscle LIM protein 1* and *LIM domain and actin-binding protein 1-like* in the claw muscles from inter-, pre- and post-molt stages were identified and further evaluated using GO and KEGG analyses, which provide the unique insight on mechanisms of the muscle's physiology changes during molting cycle. Future research will screen out and functional investigate the gene candidates, which are most directly involved in muscle growth and development induced by molting in crustacean.

Acknowledgements This work was funded by the National Natural Science Foundation of China (31572635), the Key Supporting Subject of Ecology of Shaoguan University (230079030101) and the Key Scientific Research Project of Shaoguan University. We would like to thank prof. Yongxu Cheng for his kindly arrangement for the animal sampling.

References

- Audic S, Claverie JM (1997) The significance of digital gene expression profiles. *Genome Res* 7:986–995
- Benjamini Y, Yekutieli D (2001) The control of the false discovery rate in multiple testing under dependency. *Ann Stat* 29:1165–1188
- Colbourne JK, Pfrender ME, Gilbert D, Thomas WK, Tucker A, Oakley TH, Tokishita S, Aerts A, Arnold GJ, Basu MK et al (2011) The ecoresponsive genome of *Daphnia pulex*. *Science* 331:555–561
- Das S, Pitts NL, Mudron MR, Durica DS, Mykles DL (2016) Transcriptome analysis of the molting gland (Y-organ) from the black-back land crab, *Gecarcinus lateralis*. *Comp Biochem Physiol Part D Genom Proteom* 17:26–40
- de Hoon MJ, Imoto S, Nolan J, Miyano S (2004) Open source clustering software. *Bioinformatics* 20:1453–1454
- Devaraj H, Natarajan A (2006) Molecular mechanisms regulating molting in a crustacean. *FEBS J* 273:839–846
- Dittel AI, Epifanio CE (2009) Invasion biology of the Chinese mitten crab *Eriocheir sinensis*: A brief review. *J Exp Mar Bio Ecol* 374:79–92
- El Haj AJ (1999) Regulation of muscle growth and sarcomeric protein gene expression over the intermolt cycle. *Am Zool* 39:570–579
- El Haj A, Clarke S, Harrison P, Chang E (1996) In vivo muscle protein synthesis rates in the American lobster *Homarus americanus* during the moult cycle and in response to 20-hydroxyecdysone. *J Exp Biol* 199:579–585
- Grabherr MG, Haas BJ, Yassour M, Levin JZ, Thompson DA, Amit I, Adiconis X, Fan L, Raychowdhury R, Zeng Q et al (2011) Full-length transcriptome assembly from RNA-Seq data without a reference genome. *Nat Biotechnol* 29:644–652
- Gutekunst J, Andriantsoa R, Falckenhayn C, Hanna K, Stein W, Rasamy J, Lyko F (2018) Clonal genome evolution and rapid invasive spread of the marbled crayfish. *Nat Ecol Evol* 2:567–573
- Haas AL, Baboshina O, Williams B, Schwartz LM (1995) Coordinated induction of the ubiquitin conjugation pathway accompanies the developmentally programmed death of insect skeletal muscle. *J Biol Chem* 270:9407–9412

- Huang S, Wang J, Yue W, Chen J, Gaughan S, Lu W, Lu G, Wang C (2015) Transcriptomic variation of hepatopancreas reveals the energy metabolism and biological processes associated with molting in Chinese mitten crab, *Eriocheir sinensis*. *Sci Rep* 5:14015
- Huang W, Ren C, Li H, Huo D, Wang Y, Jiang X, Tian Y, Luo P, Chen T, Hu C (2017) Transcriptomic analyses on muscle tissues of *Litopenaeus vannamei* provide the first profile insight into the response to low temperature stress. *PLoS One* 12:e0178604
- Ismail SZM, Mykles DL (1992) Differential molt-induced atrophy in the dimorphic claws of male fiddler crabs. *J Exp Zool* 263:18–31
- Kanehisa M, Araki M, Goto S, Hattori M, Hirakawa M, Itoh M, Katayama T, Kawashima S, Okuda S, Tokimatsu T et al (2008) KEGG for linking genomes to life and the environment. *Nucleic Acids Res* 36:D480–D484
- Kao D, Lai AG, Stamatakis E, Rosic S, Konstantinides N, Jarvis E, Di Donfrancesco A, Pouchkina-Stancheva N, Semon M, Grillo M et al (2016) The genome of the crustacean *Parhyale hawaiensis*, a model for animal development, regeneration, immunity and lignocellulose digestion. *eLife* 5:e20062. <https://doi.org/10.7554/eLife.20062>
- Kenny NJ, Sin YW, Shen X, Zhe Q, Wang W, Chan TF, Tobe SS, Shimeld SM, Chu KH, Hui JH (2014) Genomic sequence and experimental tractability of a new decapod shrimp model, *Neocardina denticulata*. *Mar Drugs* 12:1419–1437
- Koenders A, Yu X, Chang ES, Mykles DL (2002) Ubiquitin and actin expression in claw muscles of land crab, *Gecarcinus lateralis*, and American lobster, *Homarus americanus*: differential expression of ubiquitin in two slow muscle fiber types during molt-induced atrophy. *J Exp Zool* 292:618–632
- Kuballa AV, Holton TA, Paterson B, Elizur A (2011) Moult cycle specific differential gene expression profiling of the crab *Portunus pelagicus*. *BMC Genom* 12:147
- Lee JH, Suryaningtyas IT, Yoon TH, Shim JM, Park H, Kim HW (2017) Transcriptomic analysis of the hepatopancreas induced by eyestalk ablation in shrimp, *Litopenaeus vannamei*. *Comp Biochem Physiol Part D Genom Proteom* 24:99–110
- Li B, Dewey CN (2011) RSEM: accurate transcript quantification from RNA-Seq data with or without a reference genome. *BMC Bioinformatics* 12:323
- Li R, Li Y, Fang X, Yang H, Wang J, Kristiansen K, Wang J (2009) SNP detection for massively parallel whole-genome resequencing. *Genome Res* 19:1124–1132
- Liu L, Fu Y, Zhu F, Mu C, Li R, Song W, Shi C, Ye Y, Wang C (2018) Transcriptomic analysis of Portunus trituberculatus reveals a critical role for WNT4 and WNT signalling in limb regeneration. *Gene* 658:113–122
- Mortazavi A, Williams BA, McCue K, Schaeffer L, Wold B (2008) Mapping and quantifying mammalian transcriptomes by RNA-Seq. *Nat Methods* 5:621–628
- Mykles DL (1997) Crustacean muscle plasticity: molecular mechanisms determining mass and contractile properties. *Comp Biochem Physiol B Biochem Mol Biol* 117:367–378
- Mykles DL (1998) Intracellular proteinases of invertebrates: calcium-dependent and proteasome/ubiquitin-dependent systems. *Int Rev Cytol* 184:157–289
- Mykles DL (1999) Proteolytic processes underlying molt-induced claw muscle atrophy in decapod crustaceans. *Am Zool* 39:541–551
- Mykles DL, Skinner DM (1981) Preferential loss of thin filaments during molt-induced atrophy in crab claw muscle. *J Ultrastruct Res* 75:314–325
- Mykles DL, Skinner DM (1990) Atrophy of crustacean somatic muscle and the proteinases that do the job. A review. *J Crust Biol* 10:577
- Nakatsui T, Keino H, Tamura K, Yoshimura S, Kawakami T, Aimoto S, Sonobe H (2000) Changes in the Amounts of the Molt-Inhibiting Hormone in Sinus Glands during the Molt Cycle of the American Crayfish, *Procambarus clarkii*. *Zool Sci* 17:1129–1136
- Pickart CM, Summers RG, Shim H, Kasperek EM (2010) Dynamics of ubiquitin pools in developing sea urchin embryos. *Dev Growth Differ* 33:587–598
- Promwikorn W, Boonyoung P, Kirirat P (2005) Histological characterization of cuticular depositions throughout the molting cycle of the black tiger shrimp (*Penaeus monodon*). *Songklanakarin J Sci Technol* 27:499–509
- Qin Z, Babu VS, Wan Q, Zhou M, Liang R, Muhammad A, Zhao L, Li J, Lan J, Lin L (2018) Transcriptome analysis of Pacific white shrimp (*Litopenaeus vannamei*) challenged by Vibrio paraheemolyticus reveals unique immune-related genes. *Fish Shellfish Immunol* 77:164–174
- Saldanha AJ (2004) Java Treeview—extensible visualization of microarray data. *Bioinformatics* 20:3246–3248
- Schmiege DL, Ridgwa RL, Moffett SB (1992) Ultrastructure of autotomy-induced atrophy of muscles in the crab *Carcinus maenas*. *Can J Zool* 72:841–851
- Shean BS, Mykles DL (1995) Polyubiquitin in crustacean striated muscle: increased expression and conjugation during molt-induced claw muscle atrophy. *Biochim Biophys Acta* 1264:312–322
- Shyamal S, Das S, Guruacharya A, Mykles DL, Durica DS (2018) Transcriptomic analysis of crustacean molting gland (Y-organ) regulation via the mTOR signaling pathway. *Sci Rep* 8:7307
- Song L, Bian C, Luo Y, Wang L, You X, Li J, Qiu Y, Ma X, Zhu Z, Ma L et al (2016) Draft genome of the Chinese mitten crab, *Eriocheir sinensis*. *GigaScience* 5:5
- Spees JL, Chang SA, Mykles DL, Snyder MJ, Chang ES (2003) Molt cycle-dependent molecular chaperone and polyubiquitin gene expression in lobster. *Cell Stress Chaperones* 8:258–264
- Tian Z, Kang X, Mu S (2012) The molt stages and the hepatopancreas contents of lipids, glycogen and selected inorganic elements during the molt cycle of the Chinese mitten crab, *eriocheir sinensis*. *Fish Sci* 78:67–74
- Wang C, Li C, Li S (2008) Mitochondrial DNA-inferred population structure and demographic history of the mitten crab (*Eriocheir sensu stricto*) found along the coast of mainland China. *Mol Ecol* 17:3515–3527
- West JM (1997) Ultrastructural and contractile activation properties of crustacean muscle fibres over the moult cycle. *Comp Biochem Physiol* 117B:333–345
- West JM, Humphris DC, Stephenson DG (1995) Characterization of ultrastructural and contractile activation properties of crustacean (*Cherax destructor*) muscle fibres during claw regeneration and moulting. *J Muscle Res Cell Motil* 16:267–284
- Whiteley NM, El Haj AJ (1997) Regulation of muscle gene expression over the moult in crustacea. *Comp Biochem Phys B* 117:323–331
- Wing SS, Goldberg AL (1993) Glucocorticoids activate the ATP-ubiquitin-dependent proteolytic system in skeletal muscle during fasting. *Am J Physiol* 264:E668–E676
- Young MD, Wakefield MJ, Smyth GK, Oshlack A (2010) Gene ontology analysis for RNA-seq: accounting for selection bias. *Genome Biol* 11:R14
- Yu X, Mykles DL (2003) Cloning of a muscle-specific calpain from the American lobster *Homarus americanus*: expression associated with muscle atrophy and restoration during moulting. *J Exp Biol* 206:561–575
- Yuan J, Gao Y, Zhang X, Wei J, Liu C, Li F, Xiang J (2017) Genome sequences of marine shrimp *expopalaemon carinicauda* Holthuis

- provide insights into genome size evolution of Caridea. Mar Drugs 15(7):213. <https://doi.org/10.3390/md15070213>
- Yuan J, Zhang X, Liu C, Yua Y, Wei J, Lia F, Xiang J (2018) Genomic resources and comparative analyses of two economical penaeid shrimp species, *Marsupenaeus japonicus* and *Penaeus monodon*. Mar Genom 39:22–25
- Zhang C, Pang Y, Zhang Q, Huang G, Xu M, Tang B, Cheng Y, Yang X (2018) Hemolymph transcriptome analysis of Chinese mitten crab (*Eriocheir sinensis*) with intact, left cheliped autotomy and bilateral eyestalk ablation. Fish Shellfish Immunol 81:266–275

Publisher's Note Springer Nature remains neutral with regard to jurisdictional claims in published maps and institutional affiliations.